Proceedings of the 9ICEG
9th International Congress on Environmental Geotechnics
25-28 June, 2023 | Chania, Greece

https://doi.org/10.53243/ICEG2023-204

Characterization of aggregates derived from waste rubber and rubber-plastic blends for sustainable development

Prithvendra Singh[1], Devendra Narain Singh[2]

[1]Research Scholar, Department of Civil Engineering, Indian Institute of Technology Bombay, Mumbai 400 076, India; email: prithvendrasingh@gmail.com (ORCID ID: 0000-0001-9979-7694)

[2]PhD, FASCE, FNAE, FICE, D.L. Shah Chair Professor for Innovation, Department of Civil Engineering, Indian Institute of Technology Bombay, Mumbai 400 076, India; email dns@civil.iitb.ac.in (ORCID ID: 0000-0003-3832-1507)

ABSTRACT

Increasing quantities of discarded rubber tires have lead to various geoenvironmental and societal issues, and hence strategies for their utilization are a top priority. As the rubber in tires is crosslinked (vulcanized) with sulfur, it is highly resistant to decomposition due to chemical, thermal, biological, and photochemical activities, under ambient conditions. However, as the waste rubber tires cannot be utilized in their original form due to their non-uniform shape and size, shredding is required to create rubber aggregates (RA) that can be utilized for various geotechnical, geoenvironmental, and infrastructure projects. However, before moving ahead, the characterization of RA and their properties need to be established to understand their merits and demerits. With this in view, a comprehensive characterization of different sizes of RA has been conducted by employing sieve analysis, scanning electron microscopy, thermal & electrical properties, and load-deformation behavior. It is well understood that though particles of various sizes can be obtained by adopting the proper procedure, their specific surface area will always be lesser than the natural sands, and thus they find their utilization as drainage layers for various geoenvironmental applications. Furthermore, as expected, it has been observed that RA have better thermal and electrical insulation. Unfortunately, the stiffness of RA is less as compared to sands, and hence to come out of this limitation, the creation of rubber plastic blends (RPB) seems to be a good option. It is worth emphasizing here that as RPB are made of RA and either the commercial HDPE plastics or mix plastics from the municipal waste landfills, many of the sustainable development goals get addressed inadvertently due to waste utilization. These aggregates are expected to perform very well against thermo-mechanical-chemical loadings, as well.

Keywords: waste rubber; plastic, aggregates; cross-linked; thermal, electrical, SDGs.

1 INTRODUCTION

End-of-life tires pose serious geoenvironmental issues and have become a massive environmental burden as around 1 billion tires are being discarded annually, and around 0.5 billion are being landfilled (Rigotti and Dorigato, 2022; Tahami et al., 2019; Singh et al., 2023a). Moreover, due to the shape and impervious structure of waste rubber tires (WRT), water remains stored for an extended time, which provides a breeding habitat for mosquitos and also provides a conducive environment for rats and vermins (Rigotti & Dorigato, 2022). Furthermore, WRTs are highly resistant to chemical reagents, photochemical decomposition, biodegradation, and temperature due to their cross-linked/vulcanized structure (Mohajerani et al., 2020; Zhang et al., 2020). Unfortunately, in the case of fires, WRTs release detrimental gases and toxic volatile contaminants into the atmosphere (Mei et al., 2022; Singh et al., 2015). Mohammad et al. (2023) have reported various major fire accidents that have occurred in the *WRT* landfills. Hence, storage, handling, and disposal of *WRT*s are becoming challenging for landfill operators, municipal corporations, and rubber recyclers.

Thus, there is a dire need to utilize the WRTs in bulk, and one of the most suitable bulk utilization schemes will be their shredding to manufacture rubber aggregates (RA). These manmade aggregates have the potential to replace natural aggregates for infrastructure development and geoenvironmental applications (rubberized concrete, drainage layers, landfill cover, polymer composites, etc.)

(Anbazhagan et al., 2017; Jalal et al., 2019; Mei et al., 2022; Sridhar et al., 2009; Yaowarat et al., 2021). It should be realized that as the specific gravity of the RA is less than half the value of the natural aggregates, earlier researchers have tried to utilize the RA as lightweight fill material for infrastructure development, viz., roads, embankments, retaining walls, etc. (Akbarimehr et al., 2020; Anvari et al., 2017; Reddy & Krishna, 2017; Roque et al., 2021; Rouhanifar et al., 2020, Singh et al., 2023b). However, as expected, when loaded mechanically, the RA matrix exhibits higher deformations than that of natural aggregates. Unfortunately, the load-deformation characteristics and the micromechanical response of the *RA* both in the matrix and individual (particle) level have not been investigated by earlier researchers so far, and calls for systematic investigations. Furthermore, as expected, the RA and RPB are excellent insulation material as far as thermal and electrical loadings are concerned. Few researchers have reported the leaching of organic and inorganic contaminants from WRTs, while few reported their concentration within toxicity limits specified for tap water (Humphrey & Swett, 2006; Maeda & Finney, 2018; Selbes et al., 2015).

The utilization of RA would also facilitate to fulfill sustainable development goals, SDGs, such as (i) Good Health and Well-being (SDG-3), (ii) Industry, Innovation and Infrastructure (SDG-9), and (iii) Responsible Consumption and Communities (SDG-11) (Bodar et al., 2018; Fatimah et al., 2020) when the shredded WRTs are blended with the commercially available plastic (high-density polyethylene) to create rubber plastic blends (RPB). The RPBs so created are basically polymer composites and have a huge demand in the electronics, automobile, piping industries, etc., and day-to-day applications by the populace (viz., mobile covers, wrist-watches, earphones, etc.) (Ning et al., 2018; Sienkiewicz et al., 2017; Sripornsawat et al., 2016). However, if commercial virgin plastics could be replaced with the waste plastics retrieved from municipal waste landfills, the SDGs could be attained in a much better manner. Keeping the above-mentioned discussion in view, an attempt was made to evaluate the worthiness of RA and RPB as an alternative to the standard sands with reference to their response to mechanical, thermal, electrical, and chemical loadings.

2 MATERIALS

As the method of shredding would control the overall properties of the RA (Adhikari et al., 2019), it would have been prudent to characterize samples obtained from adopting different shredding methodologies (viz., ambient, cryogenic, water-jet, etc.). However, due to the lack of such samples, only the RA obtained from ambient grinding, and RA blended with HDPE viz., RPB (supplied by GRP Pvt. Ltd.) were used in the present study. The specific gravity of RA, RPB, and S were measured using Helium-gas pycnometer (ULTRAPYC 1200e, made by Quantachrome Instruments), and the average values was recorded as 1.21, 1.16, and 2.67, respectively. The effective size (D_{10}) of the particles considered in this study are 0.85 mm for RA and 1-2 mm for RPB, while for S, the same is >1 mm. For the sake of brevity, these details are listed in Table 1. It should be noted that three trials were performed to obtain the properties presented in Table 1. The specific surface area (SSA) reported in Table 1 (from literature) represents a range of various-size particles. The value of SSA shown for rubber and sands are for similar size particles.

Table 1. Properties of the materials used in the present study

Material	Abbreviation	G	Particle size (mm)	#SSA (m^2/g)
Rubber	RA	1.21	>0.85	0.009-0.17
Rubber-plastic blend	RPB	1.16	>1	
Sands	S	2.67	>1	1-5

#Lo Presti (2013); Shen et al. (2009); Adhikari et al. (2019); Ajayi and Horn (2017); Amoakwah et al. (2017); Padmakumar (2013)

3 EXPERIMENTAL PROCEDURE

3.1 Scanning electron microscopy

Scanning electron microscopy (SEM) was performed on the RA, RPB, and S samples after applying an ultra-thin coating (≈ 10 nm) of platinum, and high-resolution images were taken at various magnification levels to understand the surface features viz., shape, pores, etc. The instrument used for SEM is FEI Sirion Quanta 600, with an electron beam voltage range of 200 V to 30 kV.

3.2 Energy-dispersive x-ray analysis

The energy-dispersive x-ray analysis (EDAX) has been performed on the ultra-thin coated samples of RA, RPB, and S to record the spectrum of the elements from the micrographs and to estimate their elemental composition (by weight %) and the presence of leachable metals.

3.3 Load-deformation tests

The uni-directional loading has been applied to observe the load-deformation characteristics of the compacted RA, RPB, and S. The experiments were performed in a rigid mold of the cross-section 10 cm×10 cm. As expected, the deformation of the sample was noticed to be predominant just after the application of the load, and after about 10 minutes no further changes in deformation were observed. Subsequently, samples were loaded for 30 minutes, at each step loading, and the % deformation was recorded. Long-term experiments at elevated temperatures on these samples to capture their thermo-mechanical response is the future scope of this work.

3.4 Determination of thermal properties

The thermal resistivity (R_λ) of the sample was determined by using a “laboratory thermal probe”, developed based on “the transient needle method(Gangadhara Rao & Singh, 1999). The sample was prepared in an acrylic cylindrical mold (of diameter 10 cm and height 10 cm), by compacting it in 3 layers to attain the porosity (η) of 0.64, 0.58 and 0.45 for RA, RPB and S, respectively. Subsequently, the mold was closed with the top lid that contains a hole in the center to fix the thermal probe. Tests were conducted on the sample in its dry and (water) submerged states.

3.5 Determination of electrical properties

The electrical properties (viz., electrical conductivity, σ, and dielectric constant, κ) of the sample were determined by employing an impedance analyzer (Alpha A- High-Performance Frequency Analyser, Novocontrol Technologies, Germany) that works in the frequency range 1 to 10 MHz at 25±1 °C. The samples were prepared in an acrylic cuboidal mold of inner dimensions 80 mm × 59 mm × 30 mm with electrode plates of dimension 56 mm × 56 mm × 0.5 mm installed on opposite inner sides. The distance between the electrodes was maintained as 30 mm.

4 RESULTS AND DISCUSSION

4.1 Surface features and elemental composition of the particles

To understand the surface morphology of the particles, micrographs have been generated by performing SEM imaging, as depicted in Figure 1. It is evident from the micrographs that the surface morphology of particles of RA, RPB, and S are different mainly due to differences in their formation, which might be a controlling factor for their mechanical, thermal, electrical, and chemical characteristics. The fibers of polyester cord, nylon, aramid and/or rayon textiles can be seen in RA (refer to Figure 1-a), which is one of the components in rubber tires. The RA surface appears to be rough and spongy, which might be due to the ambient method of shredding of rubber tires (Adhikari et al., 2019; Lo Presti, 2013). Furthermore, the plastic coating can be seen in the case of RPB (refer to Figure 1-b). The micro-cracks are visible on the sand surface (refer to Figure 1-c), which might be due to weathering action of particles and is one of the major contributors to the grain-to-grain characteristics of the particles.

The major difference between the properties of RA and RPB is due to the difference in their composition and manufacturing type as the RPB are the blends created by mixing RA and HDPE at high temperature and shearing conditions. It will be prudent to understand the effect of coating attributes viz., thickness, roughness etc. on the properties of RPB as compared to RA. The sophisticated techniques like Fourier transform infrared spectroscopy (FTIR), nano-indentation and atomic force microscopy (AFM) might be helpful in achieving the desired objectives.

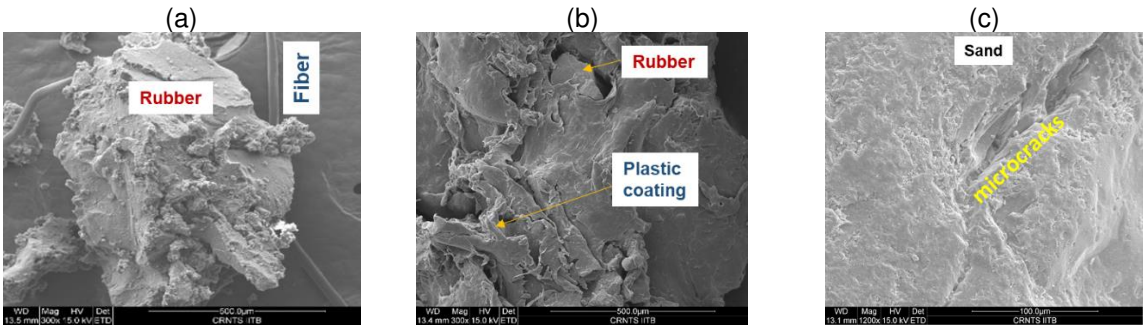

Figure 1. SEM micrographs of (a) RA, (b) RPB, and (c) S at various magnification level

Furthermore, the elemental composition of the samples for elements carbon (C), oxygen (O), Lead (Pb), zinc (Zn), silicon (Si), iron (Fe) and aluminium (Al) was obtained from EDAX as shown in Table 2. It is prudent from the Table that the content of carbon is very high in *RA* and *RPB* due to the polymeric chain of carbon. However, as expected, in S, the content of Si is the highest.

Table 2. Elemental composition of *RA*, *RPB,* and *S* obtained from EDAX mapping

Material	Elements (Weight %)						
	C K	O K	Pb M	Zn K	Si K	Fe K	Al K
RA	84.6	6.2	4.1	4.5	0.2	0.3	0.2
RPB	83	8.4	3.7	3.1	0.4	1	0.4
S	18.6	23.1	1.3	1.4	53	0.6	1.9

Note: K and M represents electron shell

4.2 Deformation in matrix after application of unidirectional loading

The step-wise unidirectional loading was applied on the matrix of RA, RPB, and S to understand the development of vertical deformation in the samples. The applied vertical stresses were selected based on the stresses prone to occur during geoenvironmental/infrastructure applications viz., leachate collection and removal systems in landfills, embankments, barrier systems etc. The vertical stresses of 50, 100, 200, 300, 400, 500, 600, 700, 800, 900 and 1000 kPa was applied, and each stress was maintained for 30 minutes. The time of 30 minutes was selected as it was observed that the vertical deformation on any particular loading achieved equilibrium and didn't change with time after approximately 10 min. The trends observed in the %strain (ε_v) vs. vertical stress (σ_v) and development of ε_v (%) with time have been presented in Figure 2-a and 2-b, respectively. From the Figure, it can be realized that the ε_v (%) is a time-dependant phenomenon at initial stresses, however, this effect gets disappear at higher stresses. The equation has been shown in Figure 2-a, which can be used to calculate the ε_v (%) for a given porosity (η). The ε_v (%) for RA and RPB are much higher as compared to that for 'S' due to the higher stiffness of natural aggregates as compared to rubber. It has been realized from this activity that the vertical stress of approximately 200 kPa seizes the vertical deformation, which needs further study by performing loading-unloading experiments and also considering other sizes of particles in the study.

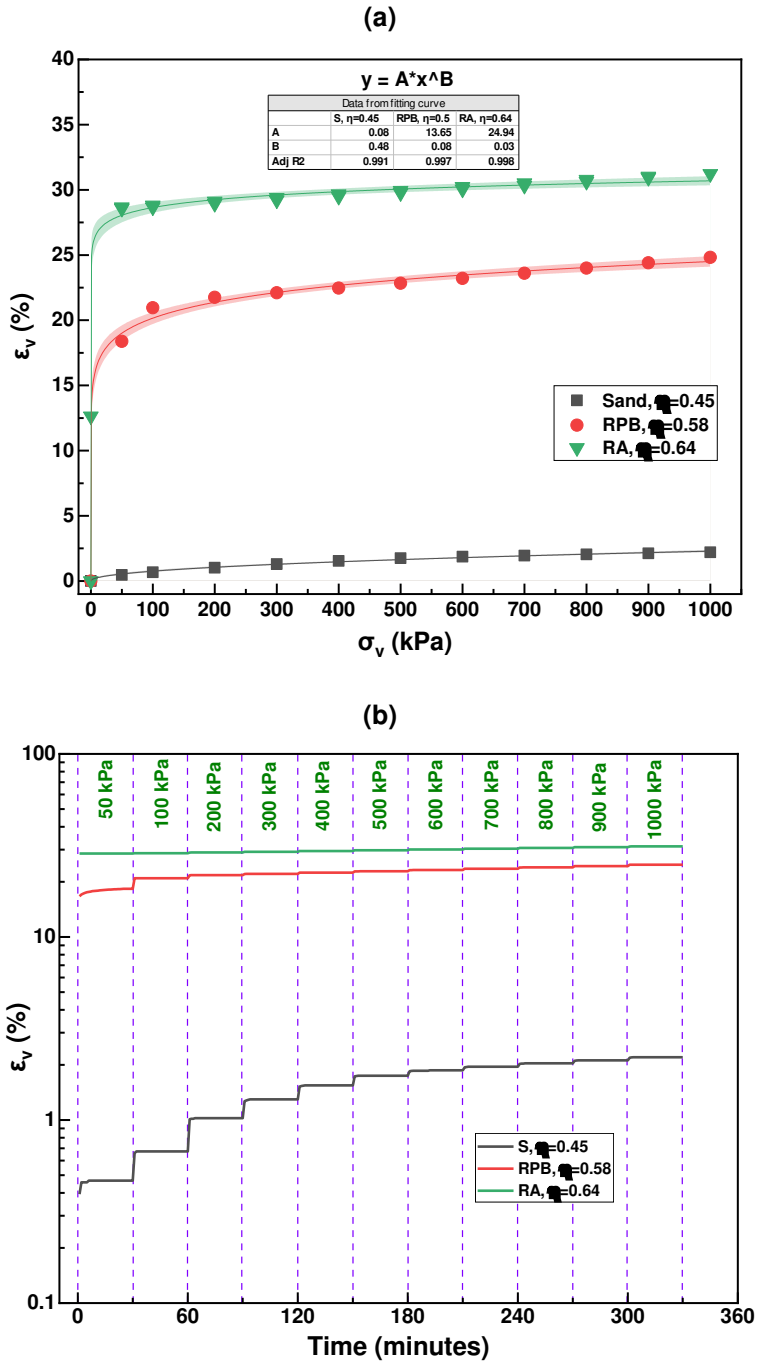

Figure 2. Variation in vertical strain (%) with (a) vertical stress, and (b) with time on RA, RPB, and S

4.3 Thermal and electrical properties of *RA*, *RPB* and *S*

The thermal properties of the materials have been calculated using the methodology elaborated in *Section 3.4*. The thermal probe was used to obtain the temperature vs. time graph. The thermal probe was calibrated for voltage and current using glycerol of known thermal resistivity for unit length of 349 °C·cm/W. The slope of the temperature vs. time graph was used to calculate the thermal resistivity of the materials (Krishnaiah & Singh, 2004). The results obtained have been presented in Figure 3-a. The dotted lines in Figure 3-a represent R_λ values of 390, 351, and 341, reported on dry sands compacted at a porosity of 0.44, 0.40 and 0.36, respectively (Krishnaiah & Singh, 2004), and the same has been

presented with dotted blue, red and purple lines. From the figure, it can be realized that the RA and RPB have higher thermal resistivity as compared to S, which proves their efficacy for insulation purposes.

Furthermore, the σ and κ of the samples was measured using the methodology mentioned in *Section 3.5*. The instrument was calibrated using standards consisting of open and short circuit corrections to eliminate unwanted impedances in series and parallel due to the cable inductance and stray capacitance, before starting the experiments. The σ and κ varies with change in frequency, and the same can be observed in Figures 3-b and 3-c. It can be concluded that the electrical properties of RA and RPB do not differ much as compared to S at a given frequency in saturated state. However, dry RPB shows least electrical conductivity and thus best suits for electrical insulation applications. Furthermore, the dielectric constant values are stable for 10^4-10^7 Hz frequency range and the values proves these materials as excellent dielectric material due to less values of dielectric constants.

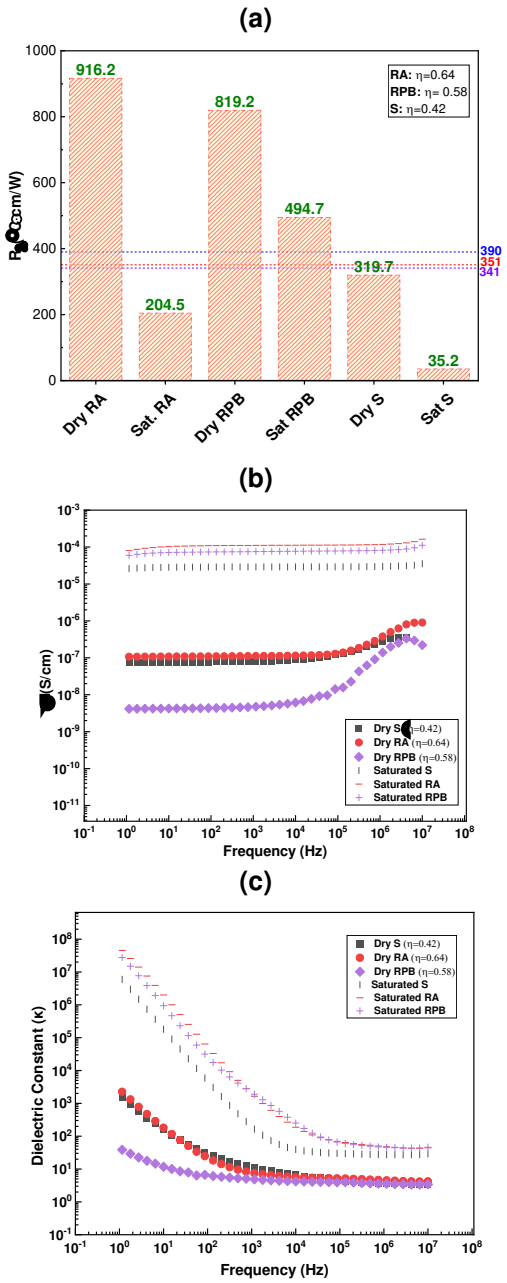

Figure 3. (a) Thermal resistivity, (b) Variation of electrical conductivity, and (c) dielectric constant with frequency on samples of *RA*, *RPB* and *S*

5 CONCLUDING REMARK AND WAY FORWARD

An effort has been made to establish the potential of rubber aggregates (RA), and rubber plastic blends (RPB), as a replacement for natural aggregates (S). It should be noted that the lesser specific surface area these aggregates make them suitable for geoenvironmental applications. The load-deformation, thermal and electrical response of RA, RPB and S has been discussed in this paper. The R_λ of dry RA and RPB are 916.2 and 819.2 °C·cm/W, respectively which proves their thermal insulation property. Furthermore, the RA and RPB have excellent property to be used as dielectric material. However, extensive research should be conducted to establish their thermo-mechanical response at elevated temperatures and extreme stresses for their application in various engineering projects such as the laying of petroleum and natural gas pipelines, water pipelines in cold regions, leachate collection systems, etc.

6 ACKNOWLEDGMENTS

The authors would like to acknowledge the help from the Sophisticated Analytical Instrument Facility (SAIF), Indian Institute of Technology Bombay, during the study. Furthermore, the authors will like to thank GRP Pvt. Ltd. for providing the rubber samples.

REFERENCES

Adhikari, J., Das, A., Sinha, T., Saha, P., & Kim, J. K. (2019). Grinding of Waste Rubber. RSC Green Chemistry, 2019-Janua(59), 1–23. https://doi.org/10.1039/9781788013482-00001

Ajayi, A. E., & Horn, R. (2017). Biochar-Induced Changes in Soil Resilience : Effects of Soil Texture and Biochar Dosage. Pedosphere: An International Journal, 27(2), 236–247. https://doi.org/10.1016/S1002-0160(17)60313-8

Akbarimehr, D., Eslami, A., & Aflaki, E. (2020). Geotechnical behaviour of clay soil mixed with rubber waste. Journal of Cleaner Production, 271. https://doi.org/10.1016/j.jclepro.2020.122632

Amoakwah, E., Frimpong, K. A., Okae-Anti, D., & Arthur, E. (2017). Soil water retention, air flow and pore structure characteristics after corn cob biochar application to a tropical sandy loam. Geoderma, 307(June), 189–197. https://doi.org/10.1016/j.geoderma.2017.08.025

Anbazhagan, P., Manohar, D. R., & Rohit, D. (2017). Influence of size of granulated rubber and tyre chips on the shear strength characteristics of sand–rubber mix. Geomechanics and Geoengineering, 12(4), 266–278. https://doi.org/10.1080/17486025.2016.1222454

Anvari, S. M., Shooshpasha, I., & Kutanaei, S. S. (2017). Effect of granulated rubber on shear strength of fine-grained sand. Journal of Rock Mechanics and Geotechnical Engineering, 9(5), 936–944. https://doi.org/10.1016/j.jrmge.2017.03.008

Bodar, C., Spijker, J., Lijzen, J., Waaijers-van der Loop, S., Luit, R., Heugens, E., Janssen, M., Wassenaar, P., & Traas, T. (2018). Risk management of hazardous substances in a circular economy. Journal of Environmental Management, 212, 108–114. https://doi.org/10.1016/j.jenvman.2018.02.014

Fatimah, Y. A., Govindan, K., Murniningsih, R., & Setiawan, A. (2020). Industry 4.0 based sustainable circular economy approach for smart waste management system to achieve sustainable development goals: A case study of Indonesia. Journal of Cleaner Production, 269, 122263. https://doi.org/10.1016/j.jclepro.2020.122263

Gangadhara Rao, M. V. B. B., & Singh, D. N. (1999). A generalized relationship to estimate thermal resistivity of soils. Canadian Geotechnical Journal, 36(4), 767–773. https://doi.org/10.1139/t99-037

Humphrey, D. N., & Swett, M. (2006). Literature Review of the Water Quality Effects of Tire Derived Aggregate and Rubber Modified Asphalt Pavement. U.S. Environmental Protection Agency (USEPA), 60. https://www.ustires.org/sites/default/files/LEA_013_USTMA.pdf

Jalal, M., Nassir, N., & Jalal, H. (2019). Waste tire rubber and pozzolans in concrete: A trade-off between cleaner production and mechanical properties in a greener concrete. Journal of Cleaner Production, 238, 117882. https://doi.org/10.1016/j.jclepro.2019.117882

Krishnaiah, S., & Singh, D. N. (2004). A Device for Determination of Thermal Properties of Soil.

Journal of Testing and Evaluation, 32(2), 114–119. https://doi.org/10.1520/jte11404

Lo Presti, D. (2013). Recycled Tyre Rubber Modified Bitumens for road asphalt mixtures: A literature review. Construction and Building Materials, 49, 863–881. https://doi.org/10.1016/j.conbuildmat.2013.09.007

Maeda, R., & Finney, B. (2018). Water Quality Assessment of Submerged Tire-Derived Aggregate Fills. Journal of Environmental Engineering, 144(2), 04017105. https://doi.org/10.1061/(asce)ee.1943-7870.0001322

Mei, J., Xu, G., Ahmad, W., Khan, K., Amin, M. N., Aslam, F., & Alaskar, A. (2022). Promoting sustainable materials using recycled rubber in concrete: A review. Journal of Cleaner Production, 373(August), 133927. https://doi.org/10.1016/j.jclepro.2022.133927

Mohajerani, A., Burnett, L., Smith, J. V., Markovski, S., Rodwell, G., Rahman, M. T., Kurmus, H., Mirzababaei, M., Arulrajah, A., Horpibulsuk, S., & Maghool, F. (2020). Recycling waste rubber tyres in construction materials and associated environmental considerations: A review. Resources, Conservation and Recycling, 155(January), 104679. https://doi.org/10.1016/j.resconrec.2020.104679

Mohammad, A., Paleologos, E. K., Ogrodnik, P., Koda, E., Osiński, P., Podlasek, A., Vaverková, M. D., Goli, V. S. N. S., Singh, P., Wang, K., Chen, X.-H., Ding, A., Jiang, N.-J., Wang, Y.-J., & Singh, D. N. (2023). Occurrence and ecotoxicological effects of fires at municipal solid waste landfills. Environmental Geotechnics, 1–12. https://doi.org/10.1680/jenge.22.00100

Ning, N., Li, S., Wu, H., Tian, H., Yao, P., HU, G. H., Tian, M., & Zhang, L. (2018). Preparation, microstructure, and microstructure-properties relationship of thermoplastic vulcanizates (TPVs): A review. Progress in Polymer Science, 79, 61–97. https://doi.org/10.1016/j.progpolymsci.2017.11.003

Padmakumar, G. P. (2013). Laboratory investigations on heat migration through soil mass [IIT Bombay]. https://www.civil.iitb.ac.in/~dns/studentdetails.html?id=25&type=PHD

Reddy, S. B., & Krishna, A. M. (2017). Tyre chips as compressible inclusions in earth-retaining walls. Proceedings of the Institution of Civil Engineers: Ground Improvement, 170(3), 137–148. https://doi.org/10.1680/jgrim.16.00034

Rigotti, D., & Dorigato, A. (2022). Novel uses of recycled rubber in civil applications. Advanced Industrial and Engineering Polymer Research, 5(4), 214–233. https://doi.org/10.1016/j.aiepr.2022.08.005

Roque, A. J., Paleologos, E. K., O'Kelly, B. C., Tang, A. M., Reddy, K. R., Vitone, C., Mohamed, A. M. O., Koda, E., Goli, V. S. N. S., Vieira, C. S., Fei, X., Sollecito, F., Vaverková, M. D., Plötze, M., Petti, R., Podlasek, A., Puzrin, A. M., Cotecchia, F., Ski, P. O., … Singh, D. N. (2021). Sustainable environmental geotechnics practices for a green economy. Environmental Geotechnics, 9(2), 68–84. https://doi.org/10.1680/jenge.21.00091

Rouhanifar, S., Afrazi, M., Fakhimi, A., & Yazdani, M. (2020). Strength and deformation behaviour of sand-rubber mixture. International Journal of Geotechnical Engineering, 00(00), 1–15. https://doi.org/10.1080/19386362.2020.1812193

Selbes, M., Yilmaz, O., Khan, A. A., & Karanfil, T. (2015). Leaching of DOC, DN, and inorganic constituents from scrap tires. Chemosphere, 139, 617–623. https://doi.org/10.1016/j.chemosphere.2015.01.042

Sienkiewicz, M., Janik, H., Borzędowska-Labuda, K., & Kucińska-Lipka, J. (2017). Environmentally friendly polymer-rubber composites obtained from waste tyres: A review. Journal of Cleaner Production, 147, 560–571. https://doi.org/10.1016/j.jclepro.2017.01.121

Singh, A., Spak, S. N., Stone, E. A., Downard, J., Bullard, R. L., Pooley, M., Kostle, P. A., Mainprize, M. W., Wichman, M. D., Peters, T. M., Beardsley, D., & Stanier, C. O. (2015). Uncontrolled combustion of shredded tires in a landfill - Part 2: Population exposure, public health response, and an air quality index for urban fires. Atmospheric Environment, 104, 273–283. https://doi.org/10.1016/j.atmosenv.2015.01.002

Singh, P., Singh, D. N., & Debbarma, S. (2023). Macro- and micro- mechanisms associated with valorization of waste rubber in cement-based concrete and thermoplastic polymer composites: A critical review. Construction and Building Materials, 371, 130807. https://doi.org/10.1016/j.conbuildmat.2023.130807.

Singh P, Goli VSNS and Singh, DN (2023b) Current practices and way forward in waste rubber utilization for Infrastructural and Geoenvironmental Engineering Applications. Environmental

Technology Reviews.

Sridhar, V., Xiu, Z. Z., Xu, D., Lee, S. H., Kim, J. K., Kang, D. J., & Bang, D. S. (2009). Fly ash reinforced thermoplastic vulcanizates obtained from waste tire powder. Waste Management, 29(3), 1058–1066. https://doi.org/10.1016/j.wasman.2008.08.013

Sripornsawat, B., Saiwari, S., Pichaiyut, S., & Nakason, C. (2016). Influence of ground tire rubber devulcanization conditions on properties of its thermoplastic vulcanizate blends with copolyester. European Polymer Journal, 85, 279–297. https://doi.org/10.1016/j.eurpolymj.2016.10.031

Tahami, S. A., Mirhosseini, A. F., Dessouky, S., Mork, H., & Kavussi, A. (2019). The use of high content of fine crumb rubber in asphalt mixes using dry process. Construction and Building Materials, 222, 643–653. https://doi.org/10.1016/j.conbuildmat.2019.06.180

Yaowarat, T., Suddeepong, A., Hoy, M., Horpibulsuk, S., Takaikaew, T., Vichitcholchai, N., Arulrajah, A., & Chinkulkijniwat, A. (2021). Improvement of flexural strength of concrete pavements using natural rubber latex. Construction and Building Materials, 282, 122704. https://doi.org/10.1016/j.conbuildmat.2021.122704

Zhang, Y., Zhang, Z., Wemyss, A. M., Wan, C., Liu, Y., Song, P., & Wang, S. (2020). Effective Thermal-Oxidative Reclamation of Waste Tire Rubbers for Producing High-Performance Rubber Composites. ACS Sustainable Chemistry and Engineering, 8(24), 9079–9087. https://doi.org/10.1021/acssuschemeng.0c02292